J. Phys.: Condens. Matter 6 (1994) L745–L753. Printed in the UK

LETTER TO THE EDITOR

Vibrational properties of copper metagermanate ($CuGeO_3$) single crystals

S D Dević†, M J Konstantinović†, Z V Popović†, G Dhalenne‡ and A Revcolevschi‡

† Institute of Physics, 11 001 Belgrade, PO Box 57, Yugoslavia

‡ Laboratoire de Chimie Solides, Université de Paris Sud, Bâtiment 414, 91405 Orsay, France

Received 27 September 1994, in final form 12 October 1994

Abstract. We present the polarized far-infrared and Raman spectra of $CuGeO_3$ single crystals in the temperature range between 10 and 300 K. Assignations of vibrational modes were performed on the basis of factor-group and normal-coordinate analyses. The frequencies of the infrared-active modes are determined using an oscillator-fitting procedure of reflectivity data. In the Raman-scattering spectra, besides phonon modes, two broad structures at about 500 and 1600 cm^{-1} are observed. The temperature dependences of the frequency, full width at half maximum (FWHM) and integrated intensities of these modes suggest their magnetic origin. In the temperature range we considered, no evidence of the spin–Peierls-transition contribution to the phonon and magnon spectra is found.

The recent discovery [1] of the spin–Peierls transition in copper metagermanate produced huge interest in investigation of the various physical properties of this material. The spin–Peierls transition occurs when a uniform Heisenberg antiferromagnetic (AF) linear chain system undergoes a transformation to a system of dimerized or alternating AF linear chains. This dimerization is mainly caused by the spin–phonon coupling between the one-dimensional spin and three-dimensional phonon systems. Until now, this effect has been discovered only in organic compounds. $CuGeO_3$ is the first inorganic material where the spin–Peierls transition has been undoubtedly observed: the temperature dependence of the magnetic susceptibility [1–4] abruptly decreases at $T = 14$ K, while neutron and x-ray measurements show [4] a second-order phase transition at the same temperature. These facts unambiguously show that $CuGeO_3$ undergoes a true spin–Peierls transition.

The crystal structure of $CuGeO_3$ is orthorhombic with unit-cell parameters given in table 1. The basic building blocks of the $CuGeO_3$ structure are corner-sharing GeO_4 tetrahedra that form chains along the c axis (figure 1). The Cu atoms are surrounded by six O atoms, forming strongly deformed CuO_6 octahedra. These octahedra, connected through short common edges, are also shown in figure 1.

The distance between Cu and O atoms in CuO_4 (squares) is 1.94 Å, a value that corresponds to the Cu–O distance in CuO_2 layers of high-T_c superconductors. The average distance between Ge and O is 1.74 Å and the distances between O atoms are from 2.54 to 2.95 Å. A detailed description of the $CuGeO_3$ crystal structure may be found in [5]. There is a disagreement about the space group of $CuGeO_3$. Namely, in [3], [6] and [7] it is stated that the space group if $Pb2_1m$ (C_{2v}^2), while in [1], [4] and [5] it is shown that $CuGeO_3$ belongs to the $Pbmm$ (D_{2h}^5) space group. Considering the analysis of the vibrational properties we will show that space group of $CuGeO_3$ is $Pbmm$ (D_{2h}^5).

0953-8984/94/480745+09$19.50

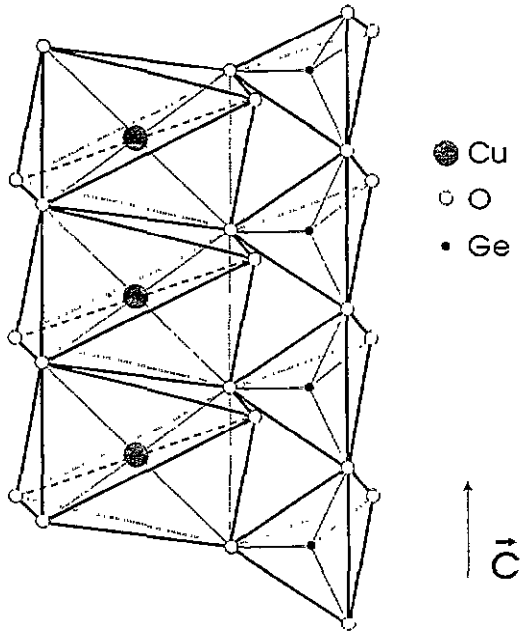

Figure 1. A schematic presentation of the $CuGeO_3$ crystal structure.

Table 1. Crystallographic parameters of $CuGeO_3$ [5].

Z	2
a (nm)	0.481
b (nm)	0.847
c (nm)	0.294
Crystal symmetry	orthorhombic
Space group	$Pbmm$ (D_{2h}^5)

Unpolarized Raman, as well as infrared (IR), transmittivity spectra of $CuGeO_3$ are measured on polycrystalline samples and most of the optical phonon frequencies [8] are determined.

This work presents polarized $CuGeO_3$ single-crystal IR and Raman spectra in a wide temperature range. The mode assignment is performed using factor-group and normal-coordinate analyses. The frequencies of TO and LO IR-active modes are determined by oscillator fitting of reflectivity data. Also, we assign Raman-active modes with magnetic origin.

The $CuGeO_3$ single crystals used in this study were cleaved from cylindrical crystals, 6 mm in diameter and 8 cm long, grown from the melt by a floating-zone method, associated with an image furnace [9]. This crucible-free technique is particularly well adapted to the growth of oxide single crystals [10] and, due to the high temperature gradients available in the solid–liquid interface during the growth process, to the fabrication of aligned composite materials [11, 12]. The single-crystal samples used here were $1.5 \times 4 \times 3$ mm^3 in size. The orientation of the principal axes was obtained by conventional Laue photographs.

The polarized far-infrared-reflection (FIR) measurements were made in the spectral range from 50 to 1000 cm^{-1} at both room and liquid-He temperature using a Bruker IFS-113v

spectrometer with a low-temperature cryostat (in the spectral range 30–650 cm^{-1}) and a Bruker IFS 66 spectrometer (for the spectral range 400–4000 cm^{-1}).

The Raman spectra were excited by the 514.5 nm line of an Ar ion laser (the average power was about 100 mW), focused to a line using a cylindrical lens. The geometry was quasibackscattering with an aperture f of the collecting objective of 1:1.4. The monochromator used was a Jobin–Yvon model U 1000 with 1800 grooves mm^{-1} holographic gratings. As a detector we used a Pelletier-effect-cooled RCA 31034 A photomultiplier with a conventional photon-counting system. The samples were held in a closed-cycle cryostat, equipped with a low-temperature controller and evacuated by a turbopump.

The $CuGeO_3$ unit cell contains two molecules, comprising 10 atoms in all (table 1). The parameters of the unit cell, originally taken from [5], were adapted to the standard setting for the *Pmma* space group. Parameters of the unit cell in this case are $a' = b = x$, $b' = c = y$, $c' = a = z$. Further analysis of the vibrational properties will proceed according to this standard setting.

The site symmetries of the atoms in the unit cell are 2d (Cu), 2e (Ge), 2f (O1) and 4i (O2). Factor-group analysis (FGA) for the *Pmma* (D_{2h}^5) space group gives 25 optically active modes [13] (table 2). Twelve of them are Raman- and 13 are IR-active modes.

Table 2. FGA of $CuGeO_3$ for the *Pmma* space group.

	Number of modes			Atoms involved	Activity	
	Total	Acoustic	Optic		Raman	IR
A_{1g}	4		4	Ge, O1, O2	xx, yy, zz	
A_u	2			Cu, O2		
B_{1g}	1		1	O2	xy	
B_{1u}	6	1	5	all		$E \parallel z$
B_{2g}	4		4	Ge, O1, O2	xz	
B_{2u}	4	1	3	all		$E \parallel y$
B_{3g}	3		3	Ge, O1, O2	yz	
B_{3u}	6	1	5	all		$E \parallel x$

The polarized room-temperature FIR spectra of $CuGeO_3$, in the spectral range from 300 to 1000 cm^{-1}, are given in figure 2. The open circles are experimental data and the full lines represent the spectra computed using the four-parameter model for the dielectric constant

$$\varepsilon = \varepsilon_\infty \prod_{j=1}^{n} \frac{\omega_{LO,j}^2 - \omega^2 + i\gamma_{LO,j}\omega}{\omega_{TO,j}^2 - \omega^2 + i\gamma_{TO,j}\omega} \tag{1}$$

where $\omega_{TO,j}$ and $\omega_{LO,j}$ are the transverse and longitudinal frequencies of the jth oscillator, $\gamma_{TO,j}$ and $\gamma_{LO,j}$ are their corresponding dampings and ε_∞ is the high-frequency dielectric constant. The best-oscillator-fit parameters are listed in table 3. The static dielectric constant, given in table 3, is obtained using the generalized Lyddane–Sachs–Teller (LST) relation

$$\varepsilon_0 = \varepsilon_\infty \prod_{j=1}^{n} \frac{\omega_{LO,j}^2}{\omega_{TO,j}^2}. \tag{2}$$

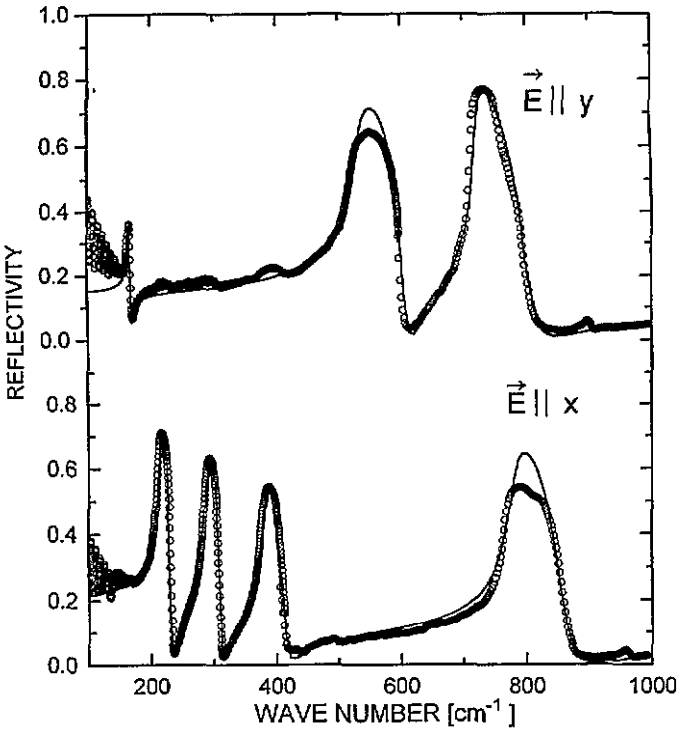

Figure 2. Room-temperature FIR spectra of $CuGeO_3$ single crystals for $E \parallel x$ and $E \parallel y$ polarizations in the spectral range 50–1000 cm^{-1}: O, experimental data; ——, calculated spectra obtained by a fitting procedure based on the model described by equation (1) with the parameters given in table 3.

Table 3. Room-temperature frequencies of IR- and Raman-active modes of $CuGeO_3$.

Mode	ω_{TO} (cm^{-1})	γ_{TO} (cm^{-1})	ω_{LO} (cm^{-1})	γ_{LO} (cm^{-1})	ε_0	ε_∞	
B_{2u}	166	3	169	3			
	530	20	602	15	5.0	3.0	
	720	9	805	35			
B_{3u}	213	6	230	5			
	287	10	310	7	6.9	3.5	
	380	12	412	17			
	777	20	860	35			
A_g	187	B_{1g}	388	B_{2g}	111	B_{3g}	117
	332				411		224
	594				712		435
	859						882

FIR spectra shown in figure 2 are obtained from the cleavage *bc* plane. In the standard setting of the D_{2h}^5 space group this plane is *xy* and, according to table 2, B_{3u} ($E \parallel x$) and B_{2u} ($E \parallel y$) symmetry modes are optically active. In the spectral region below 150 cm^{-1} there is an interference pattern, which arises because the thickness of the sample is less than 1 mm. For the $E \parallel y$ polarization, three B_{2u} modes are clearly observed. For the $E \parallel x$ polarization, four B_{3u} modes are clearly seen while the fifth mode is not observed, probably

because of its weak intensity. Due to the layered structure and splitting of the samples during the cutting, we were not able to perform measurements in $\boldsymbol{E} \parallel z$ polarization. Comparing the mode frequencies, given in table 3, with non-polarized measurements from [8], we found complete agreement. However, the remaining modes at 132, 354, 625 and 859 cm^{-1} from [8] we assigned as B_{1u} modes. These modes should be observed in $\boldsymbol{E} \parallel z$ polarization. Therefore, from 13 modes predicted by FGA we assigned four B_{1u} (132, 354, 625 and 859 cm^{-1}), three B_{2u} (166, 530, 720 cm^{-1}) and four B_{3u} (213, 287, 380 and 777 cm^{-1}) modes.

By simple comparison of spectra with IR spectra of the initial oxides, we concluded that the lowest B_{1u} mode (132 cm^{-1}) originates dominantly from Cu-atom vibrations [14] while the mode at 166 cm^{-1} originates from Ge-atom vibrations [15]. The modes with frequencies between 200 and 400 cm^{-1} are caused by Cu–(Ge)–O vibrations while the modes with frequencies larger than 500 cm^{-1} are mainly due to O-atom vibrations.

The polarized Raman spectra of a $CuGeO_3$ single crystal at room temperature are shown in figure 3.

The Raman spectrum in $z(xx)\bar{z}$ polarization is given in figure 3(a). The four A_g-symmetry modes at 187, 332, 594 and 859 cm^{-1} are clearly seen. Since the vibrations of Cu^{2+} ions do not contribute to the Raman spectra, we concluded that the 187 cm^{-1} mode originates from Ge-atom vibrations according to the corresponding normal-mode coordinate, given in table 4. The mode at 859 cm^{-1} is a stretching vibration of O atoms in GeO_4 tetrahedra, while the remaining two modes are caused by Ge–O vibrations.

Table 4. The Cartesian symmetry coordinates derived using the projection-operator technique for $CuGeO_3$ (*Pmma* space group).

Mode	Atom	Position	Normal coordinate	Mode	Atom	Position	Normal coordinate
A_g	Ge	(2e)	$z_1 - z_2$	A_u	Cu	(2d)	$y_1 - y_2$
	O1	(2f)	$z_1 - z_2$		O2	(4i)	$y_1 - y_2 + y_3 - y_4$
	O2	(4i)	$x_1 - x_2 - x_3 + x_4$				
			$z_1 + z_2 - z_3 - z_4$				
B_{1g}	O2	(4i)	$y_1 - y_2 - y_3 + y_4$	B_{1u}	Cu	(2d)	$x_1 - x_2$
							$z_1 + z_2$
					Ge	(2e)	$z_1 + z_2$
					O1	(2f)	$z_1 + z_2$
					O2	(4i)	$x_1 - x_2 + x_3 - x_4$
							$z_1 + z_2 + z_3 + z_4$
B_{2g}	Ge	(2e)	$x_1 - x_2$	B_{2u}	Cu	(2d)	$y_1 + y_2$
	O1	(2f)	$x_1 - x_2$		Ge	(2e)	$y_1 + y_2$
	O2	(4i)	$x_1 + x_2 - x_3 - x_4$		O1	(2f)	$y_1 + y_2$
			$z_1 - z_2 - z_3 + z_4$		O2	(4i)	$y_1 + y_2 + y_3 + y_4$
B_{3g}	Ge	(2e)	$y_1 - y_2$	B_{3u}	Cu	(2d)	$x_1 + x_2$
	O1	(2f)	$y_1 - y_2$				$z_1 - z_2$
	O2	(4i)	$y_1 + y_2 - y_3 - y_4$		Ge	(2e)	$x_1 + x_2$
					O1	(2f)	$x_1 + x_2$
					O2	(4i)	$x_1 + x_2 + x_3 + x_4$
							$z_1 - z_2 + z_3 - z_4$

The Raman spectra in $z(xy)\bar{z}$ and $z(xy)\bar{z}$ polarized configurations are shown in figure 3(b). Under these conditions the symmetry selection rules allow observation of only one B_{1g} mode. However, besides the B_{1g} mode at 388 cm^{-1}, the modes that belong to other crossed (B_{2g} and B_{3g}) and parallel (A_g) polarizations also appear in these spectra.

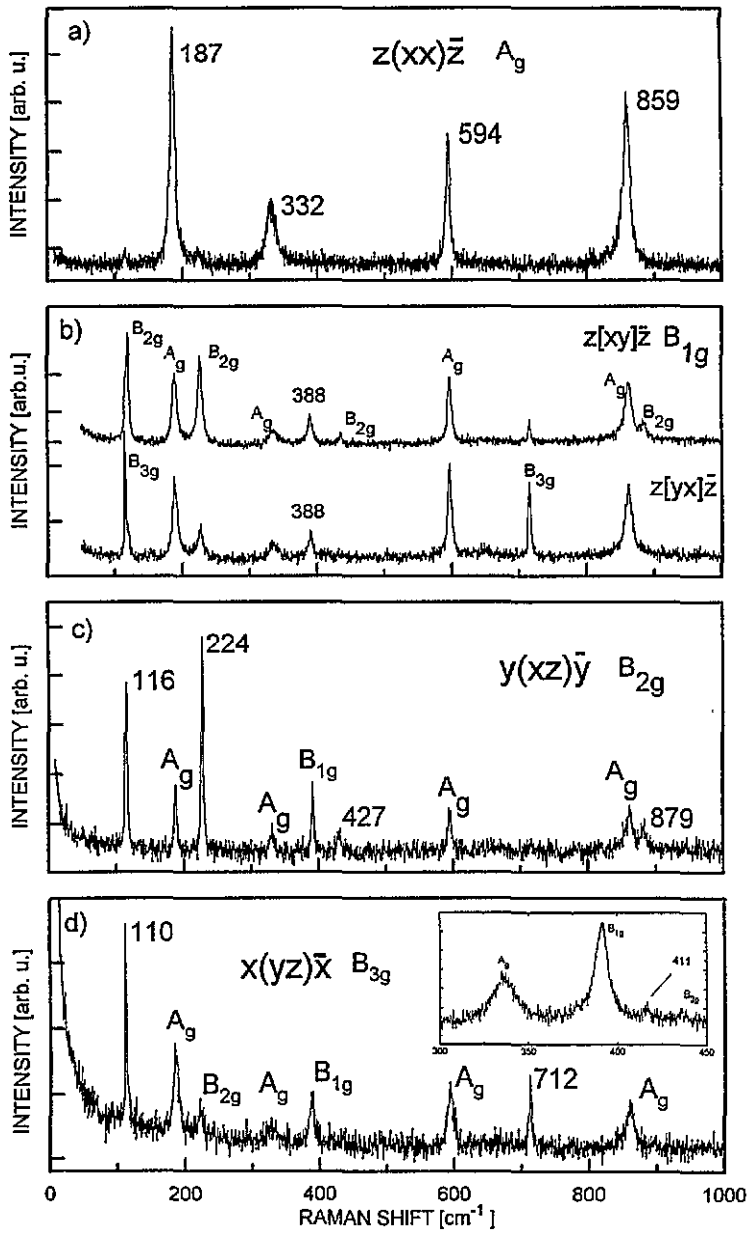

Figure 3. Raman spectra of a $CuGeO_3$ single crystal at room temperature in the spectral range 10–1000 cm^{-1} in (a) $z(xx)\bar{z}$; (b) $z(xy)\bar{z}$ and $z(xy)\bar{z}$; (c) $y(xz)\bar{y}$ and (d) $x(yz)\bar{x}$ polarizations.

We believe that the appearance of B_{2g} and B_{3g} modes together with B_{1g}-symmetry modes is due to the resonance enhancement of these modes, influenced by the 514.5 nm Ar line. In this manner the selection rules are no longer valid. Also, this 'leakage' of B_{2g} and B_{3g} modes may arise due to the imperfections of the samples in the growth direction.

The Raman spectra in $y(xz)\bar{y}$ and $x(xy)\bar{x}$ polarizations with B_{2g} and B_{3g} phonon modes are presented in figure 3(c) and (d) respectively. Comparing figure 3(b) and (d) we concluded

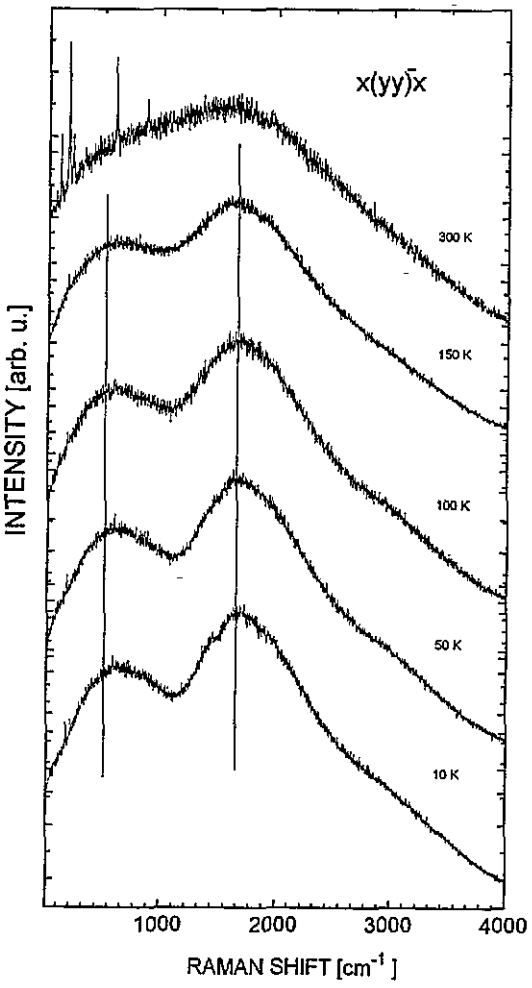

Figure 4. Polarized Raman spectra of $CuGeO_3$ at different temperatures in the spectral range 20–4000 cm^{-1}.

that the 388 cm^{-1} mode is a B_{1g}-symmetry mode, while the 116, 224, 427 and 879 cm^{-1} and 110, 411 and 712 cm^{-1} modes belong to the B_{2g}- and B_{3g}-symmetry classes, respectively. Four B_{2g} and two B_{3g} modes are clearly observed in these spectra. The third B_{3g} mode at 411 cm^{-1} is shown in the inset of figure 3(d). Its intensity is very weak compared to the intensities of the other modes from the same polarization and we resolved this mode by averaging of 20 successive spectra.

Accordingly, we assigned all twelve Raman-active modes, as predicted by FGA, with frequencies in very good agreement with [8].

The B_{1g} mode originates from out-of-phase O-atom (O2) vibrations in CuO_4 squares. Since the B_{1g} normal-mode coordinates in $CuGeO_3$ (table 4) are the same as for the B_{1g} mode in the high-T_c superconductor $YBa_2Cu_3O_7$, one can expect the appearance of these modes at similar frequencies in these materials. Actually, according to table 3, the B_{1g} mode in $CuGeO_3$ has a frequency of 338 cm^{-1}, which is very near the B_{1g} mode frequency of 340 cm^{-1} in $YBa_2Cu_3O_7$ [16].

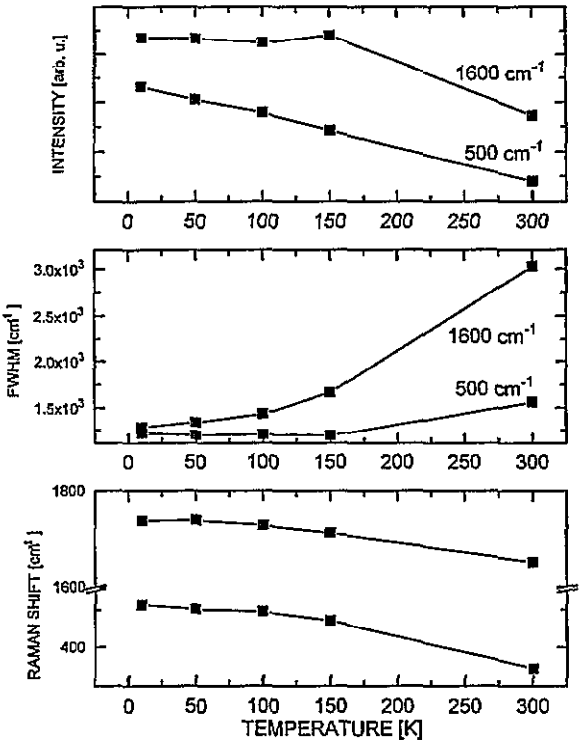

Figure 5. The intensity, FWHM and energy of two two-magnon modes as a function of temperature in the temperature range 10–300 K in $x(yy)\bar{x}$ polarization.

In the case of $Pb2_1m$ (C_{2v}^2) symmetry in $CuGeO_3$ [1,4,5], we would expect the appearance of IR- and Raman-active modes with A_1, B_1 and B_2 symmetries at the same frequencies. According to our experimental results (see table 3) this is not the case. This means that the space group of $CuGeO_3$ is not of the C_{2v} but the D_{2h} point group.

Detailed assignation of B_{2g} and B_{3g} modes will be available after the complete lattice-dynamical calculation, which is in progress.

The Raman spectra in the spectral range from 20 to 4000 cm^{-1} at various temperatures from 10 to 300 K are shown in figure 4. We obtained two broad modes centred around 500 and 1600 cm^{-1}. They appear in both $x(yy)\bar{x}$ and $x(yz)\bar{x}$ polarized configurations. A similar broad mode at 500 cm^{-1} has been previously observed by Sugai [7] and assigned as a two-magnon excitation. In addition to the 500 cm^{-1} we obtained a 1600 cm^{-1} mode that has also magnetic origin according to the intensity, full width at half maximum (FWHM) and energy dependence on temperature (figure 5). These two broad modes have very similar intensity, FWHM and frequency temperature dependences, so we concluded that they both have magnetic origin. We believe that these two excitations are due to two-magnon scattering from different points in the Brillouin zone. Better understanding of the two-magnon scattering spectra will be possible after determination of the magnon dispersion curves.

According to x-ray- and neutron-scattering studies, the $CuGeO_3$ crystal undergoes a second-order structural transition to a dimerized AF ground state at $T = 14$ K [2,4,17]. These structural transitions should produce some effects in IR-reflectivity and Raman-

scattering spectra, for example the appearance of phonon and magnon modes from the edge of the Brillouin zone due to a doubling of the crystallographic unit cell. Some additional modes have indeed been noted in the Raman spectra at a temperature of 5 K [7]. Also, IR-active modes of B_{2u} symmetry, which originate from Cu-ion vibration, may show some anomalies below the transition temperature, but our results (IR spectra at a temperature of 10 K, not presented here) show no such effects.

In conclusion, we assigned all 12 Raman-active modes (four A_g, one B_{1g}, four B_{2g} and three B_{3g}) and 11 (of 13) IR-active modes (four B_{1u}, three B_{2u} and four B_{3u} modes). Besides this, we found two broad structures in the Raman spectra and determined their frequency, FWHM and intensity temperature dependences. In the temperature region we considered (10–300 K), we found no anomalies in phonon and magnon spectra around the spin–Peierls transition temperature. The reason may lie in the fact that neutron [2, 17] and x-ray [4] experiments show pronounced anomalies at temperatures well below 14 K, outside our experimental possibilities.

We thank Z Konstantinović for help in calculating normal coordinates using the projection-operator method and W König and A Breitschwerdt for FIR and IR measurements. G Dhalenne and A Revcolevschi thank NEDO for financial support. This work was supported by the Serbian Ministry of Science and Technology under project 0104.

References

[1] Hase M, Terasaki I and Uchinokura K 1993 *Phys. Rev. Lett.* **70** 3651
[2] Nishi M 1994 *J. Phys.: Condens. Matter* **6** L19
[3] Petrakovski G A, Sablina K A, Vorotynov A M, Kruglik A I, Klimenko A G, Balayev A D and Aplesnin S S 1990 *Zh. Eksp. Teor. Fiz.* **98** 1382 (Engl. Transl. 1990 *Sov. Phys.–JETP* **71** 772)
[4] Pouget J P, Regnault L P, Ain M, Hennion B, Renard J P, Veillet P, Dhalenne G and Revcolevschi A 1994 *Phys. Rev. Lett.* **72** 4037
[5] Völlenkle H, Wittmann A and Nowotony H 1967 *Monat. Chem.* **98** 1352
[6] Ginetti Y 1954 *Bull. Soc. Chim. Belg.* **63** 209
[7] Sugai S 1993 *J. Phys. Soc. Japan* **62** 3829
[8] Adams D M and Fletcher P A 1988 *Spectrochim. Acta* A **44** 233
[9] Revcolevschi A 1970 *Rev. Int. Hautes Temp.* **7** 73
[10] Revcolevschi A and Collongues R 1969 *C.R. Acad. Sci., Paris* **266** 1767
[11] Revcolevschi A, Dhalenne G and Michel D 1988 *Mater. Sci. Form* **29** 173
[12] Revcolevschi A and Dhalenne G 1993 *Adv. Mater.* **5** 657
[13] Rousseau D L, Bauman R P and Porto S P S 1981 *J. Raman Spectrosc.* **10** 253
[14] Popović Z V, Kliche G, Konstantinović M J and Revcolevschi A 1992 *J. Phys.: Condens. Matter* **4** 10085
[15] Scott J F 1970 *Phys. Rev.* B **1** 3488
[16] Gajić R, Dević S D, Konstantinović M J and Popović Z V 1994 *Z. Phys.* B **94** 261
[17] Hirota K, Cox D E, Lorenzo J E, Shirane G, Tranquada J M, Hase M, Uchinokura K, Kojima H, Shibuya Y and Tanaka I 1994 *Phys. Rev. Lett.* **73** 736